Evaluation of Tropospheric and Mixed Single - Dual Frequency Error Models in Advanced RAIM

Juan Blanch, Todd Walter, Frank Lai

Stanford University

ABSTRACT

Advanced Receiver Autonomous Integrity Monitoring is a proposed evolution of RAIM to multi-constellation and dual frequency that is being standardized. Enabling dual frequency will have at least two effects. First, the error bounds on the pseudorange will be decreased substantially. As a result, the tropospheric residual error, which had very little effect in the user Protection Level in RAIM, will be more critical in ARAIM. Second, not all satellites will be dual frequency capable (at least initially for GPS). Only using the dual frequency satellites could result in a performance degradation compared to single frequency. To start addressing these points, in this work we: 1) evaluate the effect of tropospheric error models with correlation on ARAIM protection levels, 2) propose an implementation of mixed single frequency - dual frequency measurements and evaluate the potential performance improvements. For the first point, we find that introducing a tropospheric model with perfect correlation causes the HPL to slightly decrease in a Horizontal-ARAIM scenario and the VPL to increase by 10% in a Vertical-ARAIM scenario. For the second point, we find that introducing a mixed mode would allow users to benefit from dual frequency well before a full and redundant L1-L5 GPS constellation is available.

1. INTRODUCTION

Advanced Receiver Autonomous Integrity Monitoring (ARAIM), an evolution of RAIM to multi-constellation and dual frequency, is currently being standardized within ICAO and RTCA/EUROCAE. A reference user algorithm was part of the report describing the initial ARAIM concept developed within the bilateral US-EU Working Group C [Blanch et al. (2015), WG-C Milestone 3 Report]. This reference algorithm, which is used to evaluate the expected ARAIM performance and to support early prototyping, has been updated regularly to integrate new integrity analysis and performance improvements. For example, in Blanch et al. (2022), we proposed improvements to the baseline algorithm to improve the subset selection and to account for the temporal exposure. These changes are now in the new baseline [ARAIM ADD v4.1].

The goal of this paper is to examine possible updates to the baseline algorithm, and by extension to all ARAIM user algorithms, considering new analyses and new proposed capabilities, for two points: residual tropospheric error modeling, the mixing single frequency with dual frequency measurements.

1) *Residual tropospheric error models*. Recent work [Gallon et al., (2022)] on the tropospheric delay error has shown that the current error model specified in current aviation standards may have biases that could have a significant effect on the integrity error bounds (especially given that the margin provided by very conservative ionospheric error bounds in single frequency will disappear for dual frequency). A related concern is that the current approach treats the residual tropospheric errors as uncorrelated across pseudorange measurements. This assumption is likely conservative for the horizontal position error, but it may be optimistic for the vertical position error. After proposing error models that integrate the line-of-sight correlation and biases (similar but not necessarily identical to the ones proposed for SBAS), we evaluate their impact on the ARAIM protection levels (both vertical and horizontal) using our latest version of MAAST for ARAIM.
2) *Mixing of single frequency with dual frequency measurements*. With the current default Integrity Support Data, the ARAIM position solution and protection level will heavily lean on GPS, because it is the only constellation with a

constellation wide fault probability (P_{const}) small enough to be left unmonitored. However, reaching an L1-L5 GPS constellation that has the geometric strength of the current GPS constellation could take several years. In the meantime, ARAIM performance could be improved by mixing single frequency and dual frequency measurements. This mixing must be done with care because we must account for the receiver inter-frequency biases and for potential correlations in the residual ionospheric errors. We develop an error model that accounts for these effects and evaluate the performance benefit of enabling this mixing.

2. RESIDUAL TROPOSPHERIC ERROR MODELS

The current residual tropospheric error [MOPS] is accounted for by independent gaussian distributions in each line of sight with an elevation dependent standard deviation given by:

$$\sigma_{n,tropo}(\theta) = m(\theta) \cdot 0.12[\text{m}] \tag{1}$$

where

θ is the elevation angle in radians

$m(\theta) = \dfrac{1.001}{\sqrt{0.002001 + (\sin(\theta))^2}}$ is the obliquity factor

This model, while adequate when other errors dominate (like the residual ionospheric delay in single frequency), might be optimistic when the residual tropospheric delay accounts for a larger share of the total pseudorange error (like in dual frequency). In addition to the specific parameters used in this model (the 0.12 m standard deviation), this model does not account for the very strong correlation between the residual errors across lines of sight. A model accounting for this correlation is given by [McGraw, 2012]:

$$\varepsilon_{tropo,corr} = \underline{m}\varepsilon_{tropo,vert,corr} \tag{2}$$

In this equation, $\varepsilon_{tropo,vert,corr}$ is a scalar and $\underline{m}$ is the vector of obliquity factors. With this characterization, the covariance of the pseudorange errors is given by [McGraw, 2012]:

$$C = C_{other} + \underline{m}\underline{m}^T \sigma_{tropo,vert,corr}^{\ 2} \tag{3}$$

where C_{other} is the covariance of the remaining measurements (a preliminary description of these error terms can be found in the WG-C Milestone 3 Report with updates in ED-259A).

First, we evaluate whether the PL computed using the current model (decorrelated) would bound the positioning errors if the actual error follows the correlated model. In this case, the estimator is not matched with the measurement error covariance. To make this assessment, we compute a PL that assumes that the estimator and the detection thresholds are computed using the current model, but where we compute the covariance of the subset positions assuming the correlated model. If S is the estimator, then the covariance of the position error is given by SCS^T. Once we have the new covariances for each subset, we can compute the new protection level (PL_{corr_tropo}). A ratio of PL_{corr_tropo} /PL above one would indicate that the current PL might not be sufficiently high.

In the second analysis we compare the PLs assuming that the estimator is matched to the correlated error model. This analysis is meant to evaluate the effect that the new error model has on availability.

2.1 Advancer RAIM algorithm

Our starting point for the ARAIM user algorithm is the one described in the ARAIM ADD v4.1. For the second analysis, we modify the algorithm by changing the computation of the subset position solutions, the corresponding error covariances, and

the covariance of the solution separation statistics. For the first analysis, we will only modify the covariance of the subset solutions as indicated above. These elements are sufficient to define the ARAIM user algorithm. The PL equations remain unchanged. Although the changes are conceptually very simple, the inclusion of out of diagonal terms or a new state did require significant changes in our availability simulation tool.

2.2 Matched estimator: inverting the measurement matrix

The inclusion of the correlation introduces out of diagonal terms. For the second analysis (matched estimator) these out of diagonal terms make the inversion of the matrix more complicated compared to a diagonal matrix. However, we can use a rank one update of the inverse to minimize the associated computational load. More specifically, we have

$$C^{-1} = \left(C_{other} + \underline{m}\underline{m}^T \sigma_{tropo,vert,corr}{}^2\right)^{-1} = C_{other}{}^{-1} + \frac{\sigma_{tropo,vert,corr}{}^2}{1-\sigma_{tropo,vert,corr}{}^2 \underline{m}^T C_{other}{}^{-1}\underline{m}} C_{other}{}^{-1}\underline{m}\underline{m}^T C_{other}{}^{-1} \quad (4)$$

Because C_{other} is diagonal, the inversion of C is marginally more expensive than C_{other}. Once we have this covariance the least squares position solution is formally identical to the one using a diagonal covariance.

It is possible to formulate the above least squares with diagonal covariances by augmenting the observation equations with a virtual measurement of the residual vertical tropospheric delay. That is, we define a new geometry matrix, measurement covariance, and measurement vector as

$$\tilde{G} = \begin{bmatrix} G & \underline{m} \\ 0 & 1 \end{bmatrix},\ \tilde{y} = \begin{bmatrix} y \\ 0 \end{bmatrix},\ C = \begin{bmatrix} C_{other} & 0 \\ 0 & \sigma_{tropo,vert,corr}{}^2 \end{bmatrix} \quad (5)$$

This formulation, which is strictly equivalent to the one above, is practical because it preserves the diagonality of the measurement covariance, thus preserving the structures used to represent it (vectors instead of matrices).

2.3 Scenario definition

We evaluate the effect of the new residual tropospheric error characterization in two scenarios: a Horizontal ARAIM scenario and a Vertical ARAIM one. For both scenarios we will use the almanacs specified in the WG-C ARAIM Milestone 3 Report. For each scenario we will use the Integrity Support Data and user settings as specified in Table 1. Note that the Vertical ARAIM scenario corresponds to ISD that has not been validated and is based on preliminary values used in the WG-C ARAIM Milestone 3 Report. For H-ARAIM, the rates and probabilities reflect the current values in the draft ARAIM ICAO SARPS.

Table 1

ISD and other ARAIM parameters used in the simulations

	Horizontal ARAIM		**Vertical ARAIM**	
	GPS	**Galileo**	**GPS**	**Galileo**
σ_{URA}	2.4 m	6.0 m	1 m	1 m
σ_{URE}	2.4 m	6.0 m	1 m	1 m
b_{nom}	0.75 m	0.75 m	0.75 m	0.75 m
R_{sat}	10^{-5} /h	3×10^{-5}/h	10^{-5}/h	3×10^{-5}/h
R_{const}	10^{-8}/h	10^{-4}/h	10^{-4}/h	10^{-4}/h
P_{sat}	10^{-5}	3×10^{-5}	10^{-5}	10^{-5}
P_{const}	10^{-8}	2×10^{-4}	10^{-4}	10^{-4}
$N_{es,int}$	450		25	
$N_{es,cont}$	450		25	
T_{exp}	1 h		150 s	

Please refer to Blanch et al. 2022 for the definition of each of the entries in this table.

2.4 Effect of correlated tropospheric model on a user that assumes the decorrelated model

We computed the HPL and VPL as specified in the ARAIM ADD v4.1 (except for the updates described here) for a 10x10 lat-lon grid of users for 24 hours every 5 minutes. Figure 1 shows the ratio of the HPL with the tropospheric residual model with correlation to the baseline HPL for the H-ARAIM scenario. Figure 2 shows the corresponding plot for the V-ARAIM scenario.

We can see that the tropospheric model with correlation has a different effect in the vertical and horizontal coordinates. HPL_{tropo_corr} decreases with the correlated model. This means that assuming the correlated model is conservative in this scenario. In contrast, VPL_{tropo_corr} tends to increase (up to 12% in this case). This means that the current residual tropospheric model might need to be updated for V-ARAIM to guarantee safe VPLs.

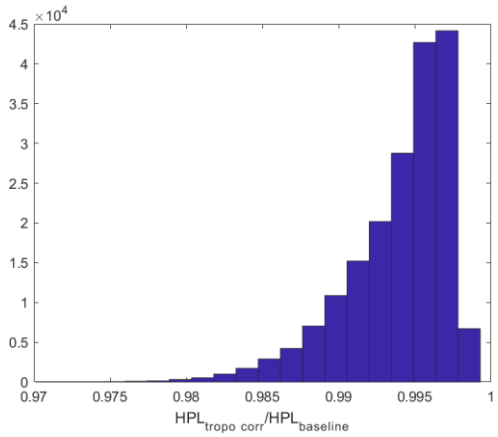

Figure 1. *Ratio of HPL_{tropo_corr} (with correlated tropospheric error) to the baseline HPL for the H-ARAIM scenario*

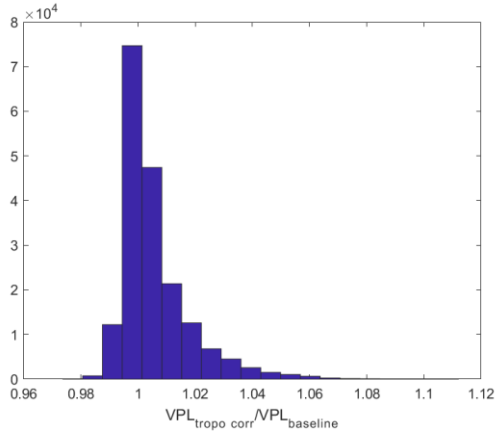

Figure 2. *Ratio of VPL_{tropo_corr} (correlated tropospheric error) to the baseline VPL for the V-ARAIM scenario*

The distinct effect on horizontal and vertical may be because, for a horizontal coordinate, the linear estimator (noted s) has the property:

$$s^T G = I \tag{6}$$

If we now rewrite the two columns corresponding to clock and vertical, we get

$$
\begin{aligned}
s^T \begin{bmatrix} 1 & \cdots & 1 \end{bmatrix}^T &= 0 \\
s^T \begin{bmatrix} \sin\theta_1 & \cdots & \sin\theta_n \end{bmatrix}^T &= 0
\end{aligned}
\tag{7}
$$

In the correlated model, the contribution to the variance of the position error is given by $\sigma_{tropo,vert,corr}{}^2 \cdot \left(s^T m\right)^2$. Using (7), we can write that for any α and β

$$
\left(s^T m\right)^2 = s^T \left(m - \alpha \begin{bmatrix} 1 & \cdots & 1 \end{bmatrix}^T - \beta \begin{bmatrix} \sin\theta_1 & \cdots & \sin\theta_n \end{bmatrix}^T \right) \tag{8}
$$

It turns out that the vector of obliquities can be roughly approximated by the linear combination of a constant and $\sin\theta$, which means that the expression in (8) is often close to zero. For the vertical coordinate, the second equation in (7) does not hold.

2.5 Effect of correlated tropospheric model on a user that assumes the correlated model (matched estimator)

Here we assume that the user applies the correlated model to compute the estimators and the thresholds (in addition to the subset position covariances). Again, we compare the new PL against the baseline as before. Note that here we are comparing two PLs that the user would be computing depending on the chosen tropospheric model. We are therefore evaluating the effect on performance, not integrity.

The matched estimator helps lower the HPLs in the H-ARAIM scenario by a small amount in most cases (Figure 3). For a few cases, there is a very small degradation (while counterintuitive, this is because the least squares estimator is not optimal for the ARAIM PL). The difference in PLs is unlikely to significantly modify the coverage at any performance level.

For the VPL in the V-ARAIM scenario (Figure 4), the use of a matched estimator helps reduce the PL, but there is still a degradation that can be as large as 10%.

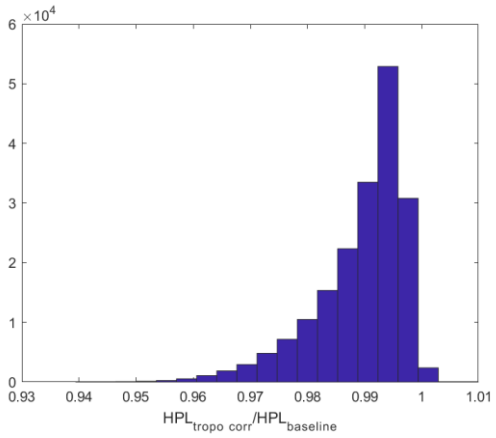

Figure 3. *Ratio of HPL_{tropo_corr} (with correlated tropospheric error and matched estimator) to the baseline HPL for the H-ARAIM scenario*

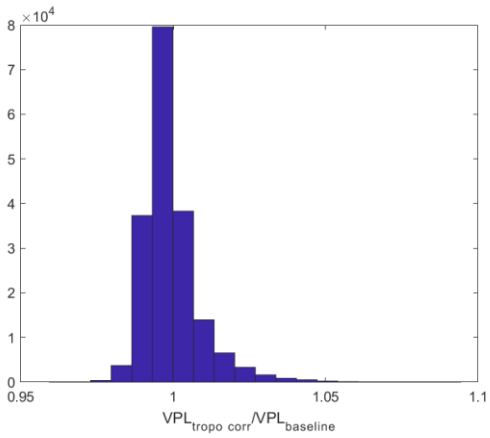

Figure 4. *Ratio of VPL_{tropo_corr} (with correlated tropospheric error and matched estimator) to the baseline HPL for the H-ARAIM scenario*

3. MIXING OF SINGLE FREQUENCY WITH DUAL FREQUENCY MEASUREMENTS

The current version of the DFMC MOPS only describes modes where all satellites use the same combination of signals (that is, either single frequency or dual frequency using the ionospheric free combination). This approach simplifies both the user algorithm and, in SBAS mode, the ground monitoring algorithms. It is however possible in principle to mix satellites with different signal combinations, especially in the case of ARAIM.

In this work, we consider a situation that reflects the current state of the GPS constellation, where a subset of the satellites does not broadcast L5 signals (Block IIR and IIR-M satellites). With this mix of satellites, it might be beneficial to add ionospheric corrections to the L1 only pseudoranges and include them in the position solution computation.

3.1 Observation equation

The pseudorange equation for the smoothed pseudorange (after applying all the corrections as described in the MOPS) can be written as follows

$$y_{L_1,k} = r_k + \delta t_{L_1} + \varepsilon_{iono,k} + \varepsilon_{L_1,cs,k} + \varepsilon_{eph\&clk,k} + \varepsilon_{trop,k} \tag{9}$$

where

r_k is the distance to the satellite

$\varepsilon_{L_1,cs,k}$ is the receiver noise and multipath error (the other errors are the residuals for the ionosphere, satellite clock and ephemeris, and troposphere)

In this equation, δt_{L_1} is the clock bias when using L1 only with ionospheric corrections. This is important because each signal will have, in effect, a different clock bias. For the L1-L5 ionospheric free combination, the measurement equation can be written

$$y_{L_1-L_5,cs,k} = r_k + \delta t_{L_1-L_5} + \frac{\gamma}{\gamma-1}\varepsilon_{L_1,cs,k} - \frac{1}{\gamma-1}\varepsilon_{L_5,cs,k} + \varepsilon_{eph\&clk,k} + \varepsilon_{trop,k} \tag{10}$$

where

$$\gamma = \frac{f_1^2}{f_5^2}$$

$\delta t_{L_1-L_5}$ is the clock bias for the L1-L5 ionospheric free combination. Let us assume that we have n_{L1L5} dual frequency measurements and n_{L1} single frequency measurements. After linearization, the observation equations can be written as follows

$$y = \begin{bmatrix} G_1 & \underline{1} & 0 \\ 0 & \underline{1} & -\underline{1} \\ G_2 & 0 & \underline{1} \end{bmatrix} \begin{bmatrix} x \\ \delta t_{L_1-L_5} \\ \delta t_{L_1} \end{bmatrix} + \begin{bmatrix} \frac{\gamma}{\gamma-1}\underline{\varepsilon}_{L_1,cs,1} - \frac{1}{\gamma-1}\underline{\varepsilon}_{L_5,cs,1} + \underline{\varepsilon}_{eph\&clk,1} + \underline{\varepsilon}_{trop,1} \\ \frac{1}{\gamma-1}\underline{\varepsilon}_{L_1,cs,1} - \frac{1}{\gamma-1}\underline{\varepsilon}_{L_5,cs,1} - \underline{\varepsilon}_{iono,1} \\ \underline{\varepsilon}_{L_1,cs,2} + \underline{\varepsilon}_{iono,2} + \underline{\varepsilon}_{eph\&clk,2} + \underline{\varepsilon}_{trop,2} \end{bmatrix} \tag{11}$$

where

x is the user position

G_1 is n_{L1L5} x 3 matrix with the lines of sight for each one of the L1-L5 measurements

The following n_{L1L5} rows are formed by the difference between the iono-free measurements and the L1 measurements

G_2 is a n_{L1} x 3 matrix corresponding to the L1 measurements lines of sight.

The geometry matrix is therefore given by:

$$G = \begin{bmatrix} G_1 & \underline{1} & 0 \\ 0 & \underline{1} & -\underline{1} \\ G_2 & 0 & \underline{1} \end{bmatrix} \tag{12}$$

3.2 Measurement covariance

For the measurement covariance we will assume that the multipath error on L1 and the multipath error on L5 are uncorrelated (this is consistent with the models specified in ED259). We will also assume that the residual ionospheric error is well characterized by a diagonal covariance. The terms in the covariance are the ones specified for RAIM in the MOPS.

The measurement covariance of the noise specified above can be computed as follows

$$\mathrm{cov}(\varepsilon) = \begin{bmatrix} \left(\frac{\gamma}{\gamma-1}\right)^2 C_{L_1,1} + \left(\frac{1}{\gamma-1}\right)^2 C_{L_5,1} + C_{trop,1} + C_{URA,1} & \frac{\gamma}{(\gamma-1)^2} C_{L_1,1} + \left(\frac{1}{\gamma-1}\right)^2 C_{L_5,1} & 0 \\ \frac{\gamma}{(\gamma-1)^2} C_{L_1,1} + \left(\frac{1}{\gamma-1}\right)^2 C_{L_5,1} & \left(\frac{1}{\gamma-1}\right)^2 C_{L_1,1} + \left(\frac{1}{\gamma-1}\right)^2 C_{L_5,1} + C_{iono,1} & 0 \\ 0 & 0 & C_{L_1,2} + C_{trop,2} + C_{URA,2} + C_{iono,2} \end{bmatrix} \tag{13}$$

The covariance of the corresponding least squares position solution is obtained using the usual formula with the geometry matrix G and the above covariance matrix. One notable difference with the current equations is the fact that the covariance of the error measurements is no longer diagonal, which could make its inversion more expensive. It is possible to make it diagonal through state augmentation, but not necessary. Instead, we can exploit the structure of the matrix. After rearrangement, it is

formed by four diagonal blocks. We can then invert the matrix block wise using the Schur complement. This approach reduces the computational load significantly compared to a standard inversion.

3.3 Advanced RAIM algorithm

As in the first section, we implement the ARAIM user algorithm is the one described in the ARAIM ADD v4.1. We update the algorithm by changing the computation of the subset position solutions, the corresponding error covariances, and the covariance of the solution separation statistics. We note that the nominal biases do not need to be applied to the measurements corresponding to the calibration of the clock biases.

3.4 Availability Results

To evaluate the potential benefits of the mixed mode, we evaluate it against the single frequency mode and the iono-free dual frequency mode. We will assume that all satellites in view can be used in the single frequency mode and only a subset of them in the dual frequency mode. The settings for the Integrity Support Data (ISD) are the ones corresponding to the default ISD specified in the draft SARPS. For GPS these parameters are given by

$$R_{const} = 10^{-8} / h$$

$$R_{sat} = 10^{-5} / h$$

$$MFD_{sat} = MFD_{const} = 1h$$

A URA of 2.4 m was assumed for all satellites. We used the GPS almanac corresponding to Week 190. In that almanac, there are 31 satellites. Of these, there are 7 Block IIR (SVNs 2, 13, 16, 19, 20, 21, 22) and 7 Block IIR-M (SVNs 5, 7, 12, 15, 17, 29, 31). In our simulations, we will assume that the 7 Block IIR have been replaced by L5 capable satellites. This means that, in our hypothetical constellation, there are 24 L1-L5 capable satellites and 7 L1 only satellites. This configuration is meant to represent a GPS constellation where we have close to a full L1-L5 constellation, but without redundancy.

We computed the FDE PL as specified in the ARAIM ADD v4.1 (also described in Blanch et al 2022) for a 10x10 lat-lon grid of users for 24 hours every 5 minutes. For each scenario, we show maps of the 99.9% HPL and the availability of 556 m HAL.

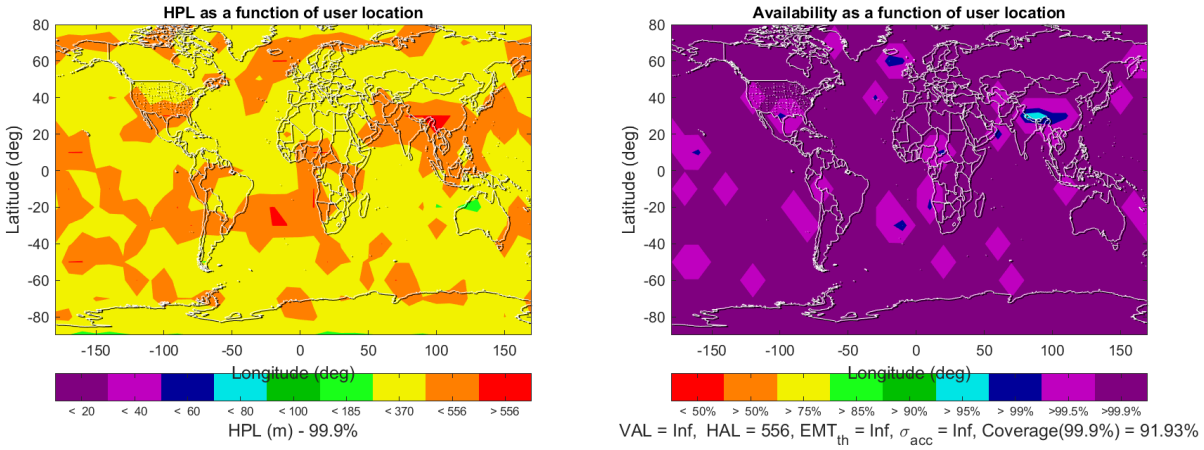

Figure 5. *99.9% HPL FDE and HAL = 556 m availability for the L1 single frequency mode. All 31 satellites are used.*

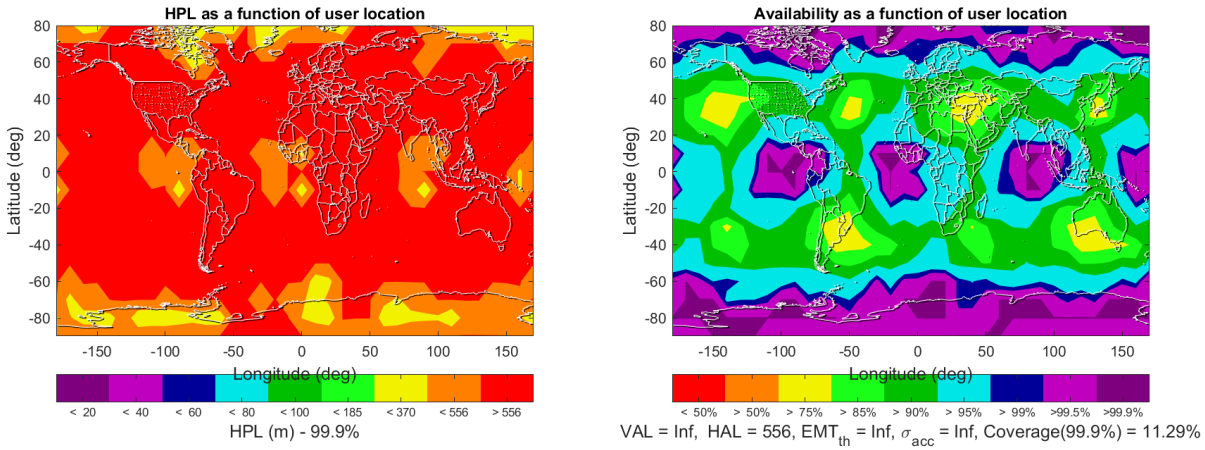

Figure 6. *99.9% HPL FDE and HAL = 556 m availability for the L1-L5 single frequency mode. Only 24 satellites are used.*

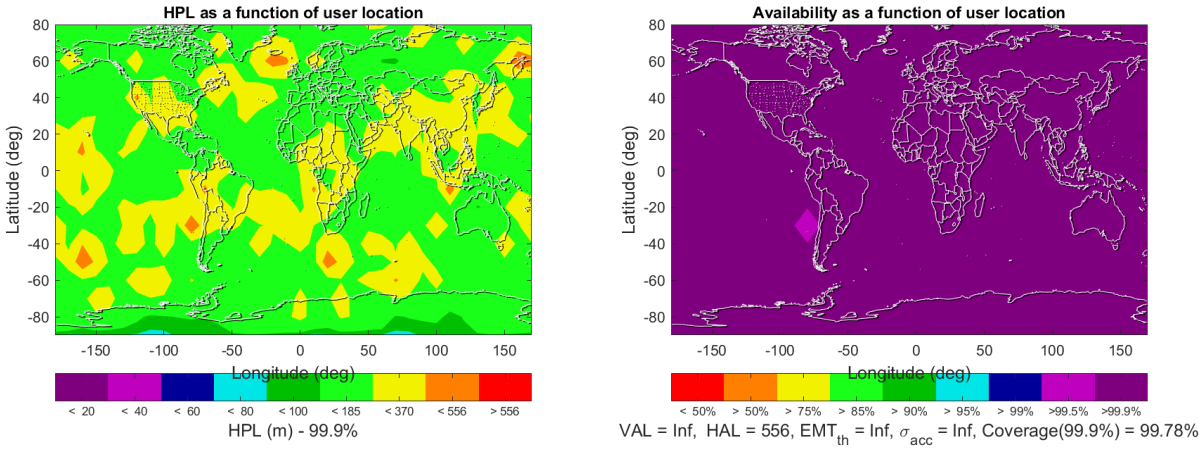

Figure 7. *99.9% HPL FDE and HAL = 556 m availability for the mixed mode. All 31 satellites are used, 24 in the L1L5 mode and 7 in the L1 mode.*

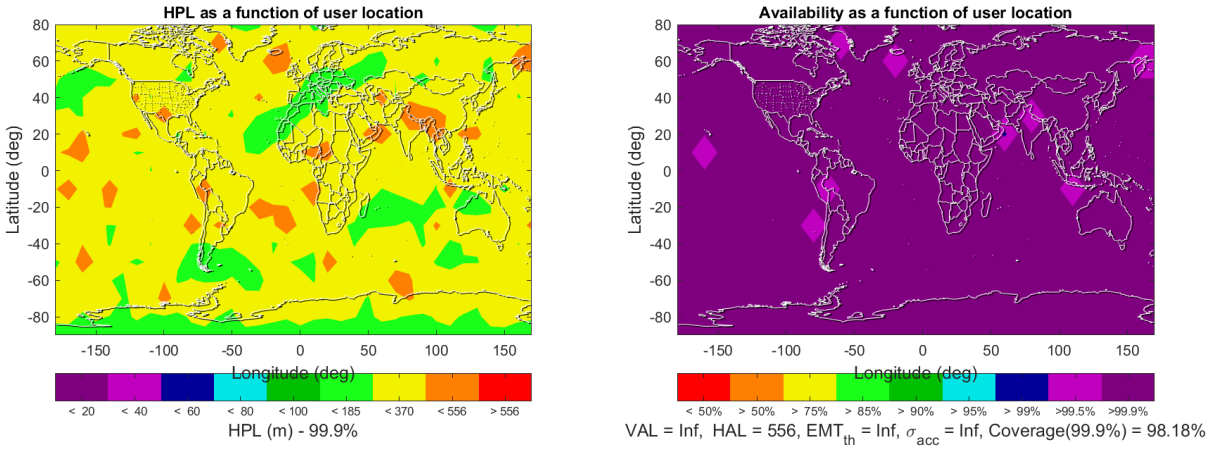

Figure 8. *99.9% HPL FDE and HAL = 556 m availability for the mixed mode. All 31 satellites are used, 17 in the L1L5 mode and 14 in the L1 mode.*

Comparing the performance Figures 5 and 6, we see that the lowered noise in the dual frequency mode does not make up for the loss in geometry strength. With the constellation assumptions made here, remaining in the L1 only mode provides better performance (for our metrics). This is not a surprising result, but it is one to consider when implementing L1-L5. Figure 7 shows that allowing the mixed mode would both drastically reduce the maximum HPLs and resolve almost all the coverage holes seen in Figure 5 (the loss of coverage is reduced from 8% to .2%, and the HPLs are halved compared to the single frequency mode). Even assuming the current configuration (Figure 8), we reduce the coverage holes from 8% to 2%.

Eventually, all GPS satellites will be L1-L5 capable, obviating the need of adding a mixed mode. However, if the transitory period is expected to last for a decade or more, it might be worthwhile allowing this mode in the DFMC standards for ARAIM.

4. SUMMARY

In this work, we have investigated two points motivated by the extension to dual frequency in ARAIM: the larger relative importance of the residual tropospheric error and the fact that, initially, not all GPS satellites will be L5 capable. For the first point, we have found that introducing a tropospheric model with perfect correlation causes the HPL to slightly decrease in a Horizontal-ARAIM scenario and the VPL to increase by 12% in a Vertical-ARAIM scenario. Therefore, while the current model is probably sufficient for H-ARAIM, it might need to be updated for V-ARAIM to guarantee integrity. For the second point, we find that introducing a mixed mode would allow users to benefit from dual frequency well before a full and redundant L1-L5 GPS constellation is available.

ACKNOWLEDGEMENTS

We gratefully acknowledge the support of the FAA Satellite Navigation Team for funding this work under Memorandum of Agreement #: 693KA8-22-N-00015.

REFERENCES

Blanch, J., Walter, T., Enge, P., Lee, Y., Pervan, B., Rippl, M., Spletter, A., Kropp, V., "Baseline Advanced RAIM User Algorithm and Possible Improvements," IEEE Transactions on Aerospace and Electronic Systems, Volume 51, No. 1, January 2015.

Blanch, J., Walter, T., Milner, C., Joerger, M., Pervan, B., Bouvet, D., "Baseline Advanced RAIM User Algorithm: Proposed Updates," Proceedings of the 2022 International Technical Meeting of The Institute of Navigation, Long Beach, California, January 2022, pp. 229-251.

Dual Frequency Multi-constellation MOPS EUROCAE ED-259A.

EUROCAE/RTCA WG2/62 Advanced RAIM Technical Subgroup Reference Airborne Algorithm Description Document v4.1. Available upon request.

https://doi.org/10.33012/2022.18254

Gallon, E., Joerger, M., Pervan, B. “Robust modeling of gnss tropospheric delay dynamics,” IEEE Transactions on Aerospace and Electronic Systems, vol. 57, no. 5, pp. 2992–3003, 2021.

Lai, F., Blanch, J., Walter, T., “Troposphere Delay Model Error Analysis With Application to Vertical Protection Level Calculation”, submitted to ION ITM 2023.

McGraw, G. A. "Tropospheric error modeling for high integrity air-borne GNSS navigation", In: Proceedings of the 2012 IEEE/ION Position, Location and Navigation Symposium, Myrtle Beach, SC,USA, 2012, pp. 158–166. https://doi.org/10.1109/PLANS.2012.6236877

Working Group C, ARAIM Technical Subgroup, Milestone 3 Report, February 26, 2016. Available at:

http://www.gps.gov/policy/cooperation/europe/2016/working-group-c/

http://ec.europa.eu/growth/tools-databases/newsroom/cf/itemdetail.cfm?item_id=8690